Ras and GTPase-activating protein (GAP) drive GTP into a precatalytic state as revealed by combining FTIR and biomolecular simulations

Till Rudack[a], Fei Xia[b], Jürgen Schlitter[a], Carsten Kötting[a], and Klaus Gerwert[a,b,1]

[a]Department of Biophysics, Ruhr-University Bochum, Universitätsstraße 150, 44801 Bochum, Germany; and [b]Chinese Academy of Sciences–Max-Planck Partner Institute for Computational Biology (PICB), Shanghai Institutes for Biological Sciences (SIBS), 320 Yue Yang Road, 200031 Shanghai, People's Republic of China

Edited by Alan R. Fersht, Medical Research Council Laboratory of Molecular Biology, Cambridge, United Kingdom, and approved August 13, 2012 (received for review March 15, 2012)

Members of the Ras superfamily regulate many cellular processes. They are down-regulated by a GTPase reaction in which GTP is cleaved into GDP and P_i by nucleophilic attack of a water molecule. Ras proteins accelerate GTP hydrolysis by a factor of 10^5 compared to GTP in water. GTPase-activating proteins (GAPs) accelerate hydrolysis by another factor of 10^5 compared to Ras alone. Oncogenic mutations in Ras and GAPs slow GTP hydrolysis and are a factor in many cancers. Here, we elucidate in detail how this remarkable catalysis is brought about. We refined the protein-bound GTP structure and protein-induced charge shifts within GTP beyond the current resolution of X-ray structural models by combining quantum mechanics and molecular mechanics simulations with time-resolved Fourier-transform infrared spectroscopy. The simulations were validated by comparing experimental and theoretical IR difference spectra. The reactant structure of GTP is destabilized by Ras via a conformational change from a staggered to an eclipsed position of the nonbridging oxygen atoms of the γ- relative to the β-phosphates and the further rotation of the nonbridging oxygen atoms of α- relative to the β- and γ-phosphates by GAP. Further, the γ-phosphate becomes more positive although two of its oxygen atoms remain negative. This facilitates the nucleophilic attack by the water oxygen at the phosphate and proton transfer to the oxygen. Detailed changes in geometry and charge distribution in the ligand below the resolution of X-ray structure analysis are important for catalysis. Such high resolution appears crucial for the understanding of enzyme catalysis.

enzyme catalysis | reaction mechanism | free energy of activation

Many cellular processes are regulated by members of the Ras superfamily. They are switched "on" by GDP-to-GTP exchange and "off" by a GTPase reaction. GTP hydrolysis is vitally important for the regulation of several signal-transduction processes in living cells (1, 2). In the case of Ras, external growth signals are transduced to the nucleus. Site-specific oncogenic mutations inhibit the GTPase reaction and the growth signal can no longer be down-regulated. This contributes to uncontrolled cell growth, eventually leading to cancer (3). Common to all members of the Ras superfamily is the catalysis of GTP hydrolysis by the G domain (4). Ras-catalyzed GTP hydrolysis is five orders of magnitude faster than in water (30 min vs. 200 d) (5). However, to control growth signals in the living cell, a further increase of five orders of magnitude in the reaction rate (30 min to 50 ms) is enabled. This is effected by GTPase-activating proteins (GAPs) that interact with Ras (6). The mechanisms of GTP hydrolysis have been extensively investigated both theoretically (7–22) and experimentally by X-ray crystallography (23–27), electron spin resonance (28–30), and FTIR spectroscopy (5, 6, 31–33).

Determination of the three-dimensional structures of Ras and GAP by X-ray crystallography represents an important milestone in the understanding of the catalysis mechanism. However, alterations of 0.01 Å in the GTP geometry, below the resolution of the X-ray structure analysis, induced by protein binding and charge shifts within GTP have been shown to contribute significantly to catalysis (16, 19). Furthermore, to prevent GTP hydrolysis during X-ray experiments, substrate analogs of GTP must be used, or data must be collected at cryogenic temperatures. The resulting protein structural models are excellent, but might lack the minor but crucial alterations within the GTP structure mentioned above. In addition, crystal contacts lead to variations within the different available Ras structural models. Depending on the crystallization conditions, Tyr32 closes (Protein Data Bank ID 3L8Z, ref. 27) or opens (Protein Data Bank ID 1QRA, ref. 26) the GTP-binding niche. FTIR difference spectra of GTP and GDP bound to Ras and Ras•GAP are complementary to X-ray structural analysis because they are obtained under more physiological conditions and are sensitive to structural details below the spatial resolution of X-ray crystallography. In principle, they are sensitive to changes in charge distribution. However, FTIR difference spectra do not provide direct, detailed three-dimensional structural information. To decode this information from the spectra, combined quantum mechanics and molecular mechanics (QM/MM) simulations can be performed. In the QM/MM simulations, crucial parts of the GTP are simulated quantum mechanically and the surrounding protein is regarded by classical MM simulations (Fig. 1). The hydrolysis from GTP to GDP is followed with millisecond time resolution by FTIR difference spectroscopy in water, in Ras, and in Ras•GAP (6). The reaction is initiated by a laser flash using caged GTP (34, 35). FTIR investigations thereby provide detailed insights into the molecular reaction mechanism (36, 37). Previous QM/MM simulations of GTP bound to Ras (16) and Ras•GAP (19), dealing with structural alterations, lacked the contribution of the magnesium ion (Mg^{2+}), which is important for the catalytic reaction (15, 21, 38). Here, in addition to the triphosphate itself, Mg^{2+}, its coordinating partners, and the ribose are treated quantum mechanically. Further, a higher level of theory is used and much longer MM simulation trajectories are simulated. In addition, we take GTP•Mg^{2+} in water into consideration. These studies focus on the investigation of the reactant ground states.

Finally, the main goal is to understand the complete reaction pathway of GTP hydrolysis in the protein environment, a great challenge for theoretical studies. The first simulations of GTP hydrolysis in Ras (7) and in Ras•GAP (9) used the empirical valence bond approach (EVB). Others used the cluster approach

Author contributions: T.R., J.S., C.K., and K.G. designed research; T.R. and F.X. performed research; T.R. analyzed data; and T.R., J.S., C.K., and K.G. wrote the paper.

The authors declare no conflict of interest.

This article is a PNAS Direct Submission.

Freely available online through the PNAS open access option.

[1]To whom correspondence should be addressed. E-mail: gerwert@bph.rub.de.

This article contains supporting information online at www.pnas.org/lookup/suppl/doi:10.1073/pnas.1204333109/-/DCSupplemental.

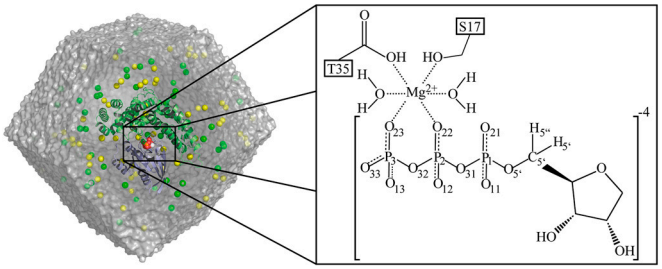

Fig. 1. Simulation. The prepared X-ray structures were relaxed by MM simulations in a water box (grey) with physiological NaCl (green and yellow spheres). The Ras•GAP (light blue and green, respectively) complex simulation system is shown. Structures equilibrated by MM were used as starting structures in QM/MM simulations. To examine charge distribution and geometry below the resolution of X-ray analysis, crucial parts of the hydrolysis reaction were treated quantum mechanically. The enlargement shows all atoms treated quantum mechanically. The rest of the protein and the solvent were treated by MM. In the QM/MM equilibration runs, the side chains of Ser17 and Thr35 and the two coordinating waters were not treated by QM. In the QM/MM production runs, the ribose was not treated by QM.

(8). Later studies used a combined QM/MM (13–15, 17, 18, 21, 22) approach with different sizes of the QM and the MM region, respectively. There is debate regarding whether the pathway is dissociative or associative (2, 17, 18, 22). Furthermore, some calculated activation energies deviate largely from experimental values. In different simulations, the energy barriers for GTP hydrolysis in Ras•GAP vary among 14 kcal/mol (1 kcal = 4.18 kJ) (14, 17), 21 kcal/mol (13, 22), and up to 70 kcal/mol (21). Of these simulations, only 14 kcal/mol (14, 17) seems reasonably close to the experimental value and therefore appears to be the most appropriate.

However, the experimental free energy of activation of 14 kcal/mol represents the intrusion of the arginine finger into the binding site, but not the hydrolysis process itself, which is simulated in the reaction path simulations. Time-resolved FTIR experiments showed that this bond breakage occurs as soon as the arginine finger intrudes into the binding niche (33). The bond breakage may have at most the same or a lower barrier. The free energy of activation of 14 kcal/mol is the upper limit, because bond breakage is not resolved experimentally.

Here, we followed a different approach. We determined the reactant GTP ground-state structures and charge distributions in water, Ras, and Ras•GAP as precisely as possible by combining QM/MM simulations and FTIR experiments. The simulations were validated by comparison of experimental and theoretical IR difference spectra. The IR difference spectra are sensitive to the geometry and charge distribution of GTP. We show that protein binding drives the GTP conformation into a precatalytic state with increased energy toward the transition state. This combination of experimental and simulated vibrational spectra provides super-resolution of the active center of an enzyme far below X-ray resolution. Such high resolution is a prerequisite to understanding enzyme catalysis.

Results and Discussion

Simulation Strategy. To determine the structure and charge distribution of GTP and Mg^{2+} in water, Ras, and Ras•GAP, we used a combination of MM and QM/MM simulations as outlined in Fig. S1. The starting structures of the MM simulations were X-ray structures in a water box with physiological NaCl. The starting structures for QM/MM simulations were six snapshots every 5 ns from the last 25 ns of the 50 ns MM trajectory. After 2.5 ps of QM/MM, vibrational modes were calculated for comparison with the experimental IR spectrum. The last 0.5 ps of the validated QM/MM trajectories were used for a detailed investigation of charge shifts and structural details of the substrate (Fig. S1). This procedure was repeated for all four simulation systems (Table S1) of solvated GTP•Mg^{2+}, Ras•GTP•Mg^{2+}, Ras•GTP•Mg^{2+}•GAP, and Ras•GDP•Mg^{2+}. For the QM/MM equilibration runs, Mg^{2+}, the atoms of the triphosphate, and the atoms of the ribose were treated quantum mechanically (Fig. 1). The rest of the protein and solvent was treated by MM. For the QM/MM production runs, Mg^{2+} and the atoms of its coordinating partner—the methyltriphosphate, the two coordinating waters, and the side chains of Ser17 and Thr35—were treated quantum mechanically.

Deduction of the Starting Structures. Direct structural information of the coordinates of GTP•Mg^{2+} in water is not available, but spectroscopic investigations (31, 39) and simulation studies (20, 38) clearly indicate a tridentate coordination of Mg^{2+} by the α-, β-, and γ-phosphates of GTP. The coordination sphere of Mg^{2+} is completed by three water molecules. Therefore, we used the GTP with a tridentately coordinated Mg^{2+} as a starting structure for the simulation of GTP•Mg^{2+} in water.

For wild-type Ras•GTP•Mg^{2+}, one X-ray structure (1QRA, ref. 26) with bound GTP is available but was taken at a cryogenic temperature; GppNHp X-ray structures 5P21 (24), 1CTQ (26), and 3L8Z (27) are also available. In all structural models, the Mg^{2+} in Ras is bidentately coordinated by the β- and γ-phosphates and the nonbridging oxygen atoms of the β- and γ-phosphates are in an eclipsed position. Thr35 and Ser17 of Ras coordinate the Mg^{2+} and two water molecules. The important roles of Lys16, Gly13, and Gly15 in stabilizing the nucleotide are extensively discussed in the literature (4, 23, 24, 26, 40). Lys 16 stabilizes the γ- and β-phosphate by hydrogen bonds to O_{12} and O_{33}, and Gly13 and Gly15 form hydrogen bonds to either the O_{32} or O_{12} of the β-phosphate. However, there is a debate on the position of Tyr32. In the X-ray structure 1QRA (26), the Tyr32 is not hydrogen-bonded to the γ-phosphate, and the binding niche is open. However, an analysis of the crystal contacts reveals that the Tyr32 has a hydrogen bond to O_{13} of the γ-phosphate of the neighboring Ras protein. Therefore, this open structure could also be an artifact of crystallization. Such a hydrogen bond between the Tyr32 and the neighboring Ras protein is also seen in the more recent GppNHp X-ray structures: 5P21 (24) and 1CTQ (26). However, in the latest structure, 3L8Z (27), the binding niche is closed by Tyr32. In 1QRA (26), 5P21 (24), and 1CTQ (26), the crystallization symmetry is the same, with *P* 32 2 1 as the symmetry operator for the space group. In 3L8Z (27), a different crystallization symmetry was observed with *H* 3 2 as the symmetry operator for the space group. Our MM simulation studies show that the closed structure is energetically preferred and the calculated vibrational spectrum fits better to the experimental one (38). Additionally, electron spin resonance (29) and FTIR spectroscopic investigations (41) confirm the closed structure. In summary, there is strong evidence for the Tyr32 closed structure. The open structure appears to be a crystallization artifact. Therefore, we considered only the closed structure for further simulations.

No GTP-bound X-ray or NMR structure is available for the Ras•GAP complex. Therefore, most of the theoretical studies (14, 19, 38) used the X-ray structure, 1WQ1 (25), of Ras GDP•AlF_3 GAP, which represents a transition-state analog, and exchanged GDP•AlF_3 with GTP as an approximation of the GTP state. We followed the same approach. The general coordination of Mg^{2+} is the same as in Ras alone, but the distances between Mg^{2+} and its coordinating partners in the Ras protein are smaller (38). The main changes in coordination result from the intruding arginine finger (Arg789), which displaces the Tyr32 and forms hydrogen bonds with O_{13} of the γ-phosphate and to O_{11} of the α-phosphate. It has been shown that, once the arginine finger moves into the binding niche, bond cleavage occurs immediately (33).

Validation. We used the X-ray structural models as the initial structures for our MM and subsequent QM/MM simulations. The protein was relaxed in a more native environment in solution with physiological conditions and temperature. Possible artifacts in the X-ray structure, such as crystal contacts, could be identified and relaxed as previously described for the Tyr32 in Ras (38). However, the resulting GTP structure might still be flawed by inappropriate simulation parameters or a start structure caught in an unfavorable local minimum by high-energy barriers. Therefore, the accuracy was validated by comparison with experimental data. Here, as a benchmark for the accuracy of the simulation, the simulated and measured IR difference spectra of GTP and GDP bound to Ras and Ras•GAP were compared (Fig. 2). IR spectra are sensitive to geometry and charge shifts. The simulated difference spectrum reveals only the phosphate vibrations, whereas the experimental spectrum includes the vibrations of all molecular groups that change during hydrolysis, including those of Ras and Ras•GAP. Here, we compared the region between 850 and 1,300 cm^{-1}, where the phosphate vibrations mainly appear. However, the band of the appearing P_i (Fig. 2, grey-hatched band) cannot be seen in the simulated spectra because the released P_i is not included in the simulation system. The calculated intensities were normalized. The calculated bandwidth represents the standard deviation of the frequencies caused by inhomogeneous broadening in the six snapshots for each state. In contrast to other studies (42–44) that did not consider vibrational modes of phosphates, our vibrational modes were calculated without a scaling factor. Studies concerning vibrational modes of phosphate groups do not apply scaling factors, and the observed rmsds between calculated vibrational modes and the available experimental values were 22 cm^{-1} (20), 25 cm^{-1} (45), or 34 cm^{-1} (19). Here, we obtained a rmsd of 24 cm^{-1} between theory and experiment for Ras•GTP and 22 cm^{-1} for Ras•GDP (Table S2). Small structural changes resulted in observable changes in the calculated spectrum (38). To better compare the bandwidth and relative positions between the GTP and GDP states, we imposed a 20-cm^{-1} shift to higher wavenumbers on simulated vibrational modes below 1,150 cm^{-1}. The shift of 20 cm^{-1} is about 2% of the wavenumber, within the error of the method. The overlay of the simulated and measured IR difference spectra in the phosphate region shows good agreement in bandwidth and intensity (Fig. 2). This comparison shows that GTP and GDP bound to Ras are correctly simulated. Similar agreement was observed for GTP•Mg^{2+} in water and Ras•GAP (Table S3). Rudack et al. (38) provided a detailed analysis of each of the vibrational modes. Note, that the experimental spectrum for Ras•GTP•Mg^{2+}•GAP is observed from a structure in which the arginine finger is outside the binding niche. Bond breakage occurs as soon as the arginine finger intrudes on the binding site. Therefore, the precatalytic structure with the arginine within the binding site, and from which the vibrational modes are calculated, cannot be resolved by FTIR spectroscopy (33). In our simulations the arginine forms a strong hydrogen bond to the γ- and α-phosphate, which may explain the difference between theory and experiment for the vibrational modes $\nu_a(PO_3)_\gamma$ (1,206/1,157 cm^{-1}) and $\nu_a(PO_2)_\alpha$ (1,247/1,260 cm^{-1}) (38).

These data show that the geometry and charges in the simulated GTP and GDP structures are as precise as the FTIR experimental data of GTP and GDP within an error of only 2%. The following conclusions can be drawn regarding the catalysis based on the observed changes in geometry and charge shifts within GTP going from GTP•Mg^{2+} to Ras•GTP and Ras•GTP•GAP.

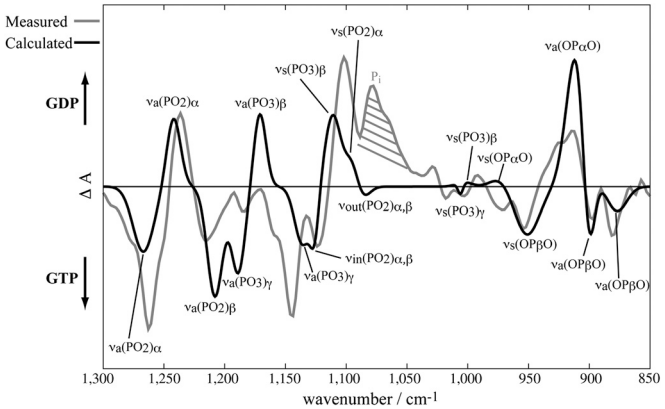

Fig. 2. Comparison of theoretical and experimental difference spectra of Ras•GTP•Mg^{2+} and Ras•GTP•Mg^{2+}. To compare directly the bandwidth and relative positions between the GTP and GDP states, we imposed a 20-cm^{-1} shift to higher wavenumbers on the simulated vibrational modes below 1,150 cm^{-1}. The vibrational modes were calculated without a scaling factor. The intensities are normalized. The calculated bandwidth is the standard deviation of the frequencies caused by the inhomogeneous broadening taken from six snapshots for each state. The overlay reveals good agreement between theory and experiment for bandwidth and intensity. The grey-hatched band in the experimental spectrum is evoked by the P_i, which is not included in the simulation and therefore cannot be observed in the calculated spectra. Detailed frequencies are given in Table S1.

Acceleration by Destabilizing the Reactant Structure. Complexation of GTP•Mg^{2+} with Ras induces a change from tridentate coordination of Mg^{2+} in water (Fig. 3*A*) to a bidentate coordination

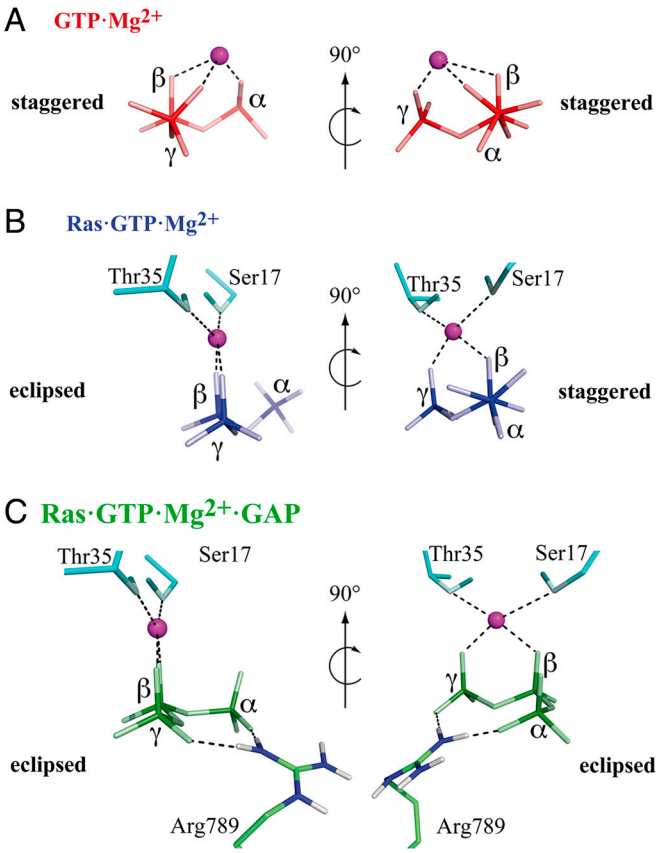

Fig. 3. Changes in the triphosphate conformation that accelerate hydrolysis by destabilizing the reactant state. Shown on the left is the triphosphate with the perspective along the axis through the γ- and the β-phosphate. Shown on the right is the triphosphate with the perspective along the axis through the α- and the β-phosphate. The protein environment of Ras changes the conformation of GTP•Mg^{2+} from a staggered position of the nonbridging oxygen atoms of β- and γ-phosphate in water (*A*) to an eclipsed one in Ras (*B*). In the Ras•GAP complex (*C*), the intruding arginine finger of GAP further leads to an eclipsed position of the β- and α-phosphates.

in Ras (Fig. 3*B*). This rotates the γ- and β-phosphates from an antiplanar (afterwards denoted as staggered) conformation in water to a coplanar (afterwards denoted as eclipsed) conformation in Ras. A value of the dihedral O_{23}–P_3–P_2–O_{22} of ±45° indicates a staggered position, whereas 0° indicates an eclipsed position. For GTP in water we observe −42°, and in Ras, −16°, or an almost-eclipsed conformation. This agrees with the X-ray structural models of GTP bound to Ras (24, 26, 27), and reveals that this energetically unfavorable GTP conformation observed at cryogenic temperatures is not an artifact caused by freezing at low temperature but still prevails under physiological conditions. The eclipsed conformation of the negatively charged oxygen atoms is energetically less favorable because it causes repulsion between the γ- and β-phosphates. Thereby, the educt state is destabilized and shifted closer to the transition state. The rotation of β- and γ-phosphate groups from a staggered to an eclipsed conformation appears to be crucial for the catalysis.

The arginine finger plays a key role in Ras•GAP catalysis, as elucidated by Scheffzek et al. (25). In the simulated structural model here, the arginine forms a hydrogen bond to the α- and γ-phosphates (Fig. 3*C*) and rotates the α-phosphate towards an eclipsed conformation with respect to the β-phosphate. The dihedral O_{22}–P_2–P_1–O_{21} changes from −46° in Ras to −2° in Ras•GAP. Now all three phosphates are in an eclipsed position. This was not observed in the X-ray structural model of the transition-state analog of AlF_3•GDP. In this structural model, the conformation of the β-phosphate with respect to the α-phosphate remains staggered as in Ras. Beside the fact that this structure is resolved with a GTP analog, the resolution is 2.5 Å instead of 1.6 Å as in Ras•GTP. The change between staggered and eclipsed is below the resolution of the Ras•GAP X-ray structure.

Two more changes in geometry below the resolution of X-ray analysis drive the triphosphate structure closer to the transition state. The bond between the phosphorous atom of the γ-phosphate (P_3) and the oxygen atom (O_{32}) of the β-phosphate, which is cleaved, is elongated (Fig. 4) from 1.73 Å in water to 1.74 Å in Ras, and 1.76 Å in Ras•GAP (38). The elongation in Ras is evoked by repulsion of the eclipsed nonbridging oxygen atoms of the γ- and β-phosphates. In Ras•GAP, the intruding arginine finger causes additional elongation. Energetically, a shift of 0.02 Å in bond length is significant.

Because of the combined effects of bond elongation and the attraction of Mg^{2+} on the O_{23}, the γ-phosphate becomes more planar, as demonstrated by a decrease in the O_{23}–P_3–O_{32} angle from 105.1° in water to 104.9° in Ras and 104.1° in Ras•GAP (38). This facilitates the nucleophilic attack.

Acceleration by Changes in Charge Distribution. Changes in geometry induce changes in charge distribution. The partial charge of the P_3 of the γ-phosphate becomes more positive, from +1.39 e_0 in water (Fig. 4*A*) to +1.43 e_0 in Ras (Fig. 4*B*), and +1.46 e_0 in Ras•GAP (Fig. 4*C*). Overall, the whole γ-phosphate group becomes more positive, whereas two oxygen atoms, O_{13} and O_{33}, of the γ-phosphate remain negative at around −1.00 e_0. The increased positivity of the γ-phosphorous atom facilitates nucleophilic attack by the oxygen atom of the water molecule, as required for hydrolysis. One of the two negatively charged oxygen atoms of the γ-phosphate serves as the target for the transfer of a proton from the attacking water to the γ-phosphate. This agrees with recent studies (22) that identified O_{13} as the target for the proton transfer.

Analysis of the Conformational Energy. As long as the transition states for GTP•Mg^{2+} in water and in Ras are unknown, and possibly even different, we cannot compare in detail the activation free energy of GTP•Mg^{2+} hydrolysis in water to that of GTP•Mg^{2+} bound to Ras. However, the situation is different comparing GTP hydrolysis in Ras and Ras•GAP, which might have similar transition states. Here, the conformation and coordination of GTP in both protein environments differ only in details (Fig. 5). To analyze qualitatively the energetic consequences of changes in geometry and charge distribution, we estimate the self-consistent field energy of the triphosphate Mg^{2+} moiety in a vacuum. The averaged structure of the triphosphate Mg^{2+} moiety is extracted from the six equilibrated QM/MM simulations in Ras and Ras•GAP. Their energies are calculated by QM. The conformational energy of GTP bound to Ras•GAP is 28 kJ/mol higher than that of GTP bound to Ras. It seems that the increase in conformational energy drives GTP even closer to the transition state, and thereby reduces the free energy of activation by 28 kJ/mol (approximately 6.7 kcal/mol). Indeed, the experimentally determined difference in the activation free energy for hydrolysis in Ras (30 min) and in Ras•GAP (50 ms) is ≤26 kJ/mol (approximately 6.2 kcal/mol), which agrees with our calculations (Fig. 5). Of course, our result represents only an estimate because the contribution of the entropy is not included in our analysis.

Furthermore, Ras is a regulatory protein and not a typical enzyme optimized for efficient substrate turnover. For the latter, destabilization of the reactant state could lead to less substrate binding, which would lower the turnover. In this case, the energy of the complete substrate, especially the binding energy, must be considered. To stop signal transduction of Ras, only the GTP hydrolysis, but not substrate binding, must be considered. Thus, we analyzed only the energy of the triphosphate Mg^{2+} moiety and not the complete GTP. The increase of the energy of the triphosphate Mg^{2+} moiety can efficiently contribute to catalysis, as shown here. In summary, the increase in conformational energy of GTP is a major contributor to catalysis.

Conclusion

Ras changes the conformation of GTP•Mg^{2+} from a staggered position of the nonbridging oxygen atoms of β- and γ-phosphates in water to an eclipsed conformation (Fig. 5). The change is caused by the change in triphosphate coordination of the Mg^{2+} from tridentate in water to bidentate forced by Ras. Additionally,

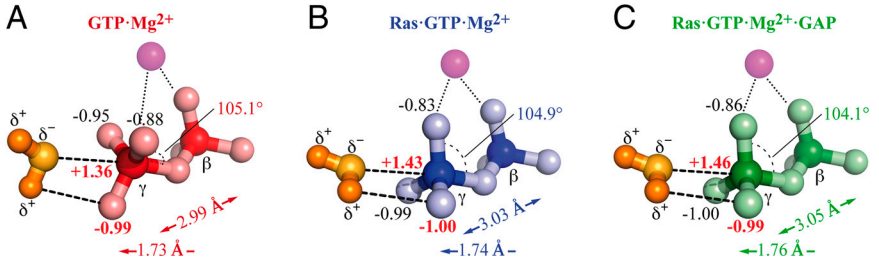

Fig. 4. Changes in charge distribution and structure of the triphosphate that accelerate hydrolysis. The γ-phosphate becomes more positive, facilitating the positioning of the negatively charged oxygen of the attacking water, and two of the nonbridging oxygen atoms of the γ-phosphate remain negative, presenting possible targets for proton transfer. The bond between P_3 and O_{32} that is cleaved during hydrolysis is lengthened, and the γ-phosphate group becomes more planar. These effects already occur in Ras and are amplified by complex formation with GAP. All partial charges are given in the unit of the electron charge, e_0.

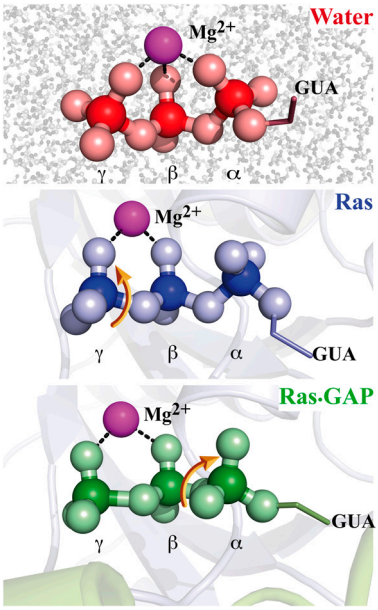

Fig. 5. Changes in geometry and charge responsible for catalyzing the increase in GTP hydrolysis by 10 orders of magnitude. The Ras protein forces GTP into a conformation with a conformational energy 154 kJ/mol higher than that of GTP in water. This is effected by a change from the staggered to the eclipsed positioning of the nonbridging oxygen atoms of the γ- and β-phosphates (induced by the change from an α-, β-, and γ-phosphate–coordinated Mg^{2+} in water to a β- and γ-phosphate–coordinated one in Ras), as well as an elongation of the bond between P_3 and O_{32} that is cleaved during hydrolysis, and the γ-phosphate group's becoming more planar. These effects are amplified by the intruding arginine finger of GAP, and the nonbridging oxygen atoms of the α- and β-phosphates are also rotated into an eclipsed position. These lead to a further 28 kJ/mol increase in the conformational energy of GTP bound to Ras•GAP compared to GTP bound to Ras. This is similar to the experimentally determined 26 kJ/mol difference in the free energies of activation for hydrolysis in Ras (30 min) and in Ras•GAP (50 ms). This indicates acceleration by a factor of 10^5 from Ras to Ras•GAP and by 10^{10} from water to Ras•GAP.

the intruding arginine finger of GAP induces an eclipsed position of the β- and α-phosphates. The conformational change of the nonbridging oxygen atoms from a staggered to an eclipsed position lengthens the bond between P_3 and O_{32}, which is cleaved during hydrolysis, with the γ-phosphate group becoming more planar. Concomitant changes in charge distribution facilitate the nucleophilic attack by a water molecule (Fig. 4): The γ-phosphate becomes more positive, facilitating the positioning of the negatively charged oxygen of the attacking water, and two of the nonbridging oxygen atoms of the γ-phosphate remain negative and are possible targets for proton transfer. All these effects already occur going from GTP•Mg^{2+} in water to Ras and are amplified by GAP. In summary, these changes lower the barrier for hydrolysis by raising the conformational energy of GTP in the reactant state, driving it closer to the transition state (Fig. 5). The difference in the conformational energies of the triphosphate Mg^{2+} moiety bound to Ras and Ras•GAP is about 28 kJ/mol, in excellent agreement with the energy necessary (≤26 kJ/mol) to accelerate hydrolysis by a factor of 10^5 in Ras•GAP compared to intrinsic Ras.

Detailed insight into the catalysis of GTP hydrolysis by Ras and Ras•GAP is gained by the combination of X-ray, FTIR, and QM/MM simulations. This provides very high resolution of the structure and charge distribution of the enzyme-bound ligand well below X-ray structural resolution, accompanied by changes in charge distribution. These data are crucial for understanding catalysis in proteins.

Methods

Simulation Setup. MM simulations were performed with GROMACS 4.0.7 (46, 47), and QM/MM simulations with GROMACS/Gaussian03 (47–49) and GROMACS/CPMD (47, 50, 51). Hydrogens were added to the X-ray structures and the structures checked and amended with the MAXIMOBY algorithm (52). Parameters for the MM and QM/MM simulations were as described by Rudack et al. (38).

Conformational Energy Calculation. To calculate differences in the conformational energies of the triphosphate in water, Ras, and Ras•GAP, we took the average structure of the GTP with the coordinated Mg^{2+} over the last 500 ps of six snapshots for each environment. The nucleoside was replaced by a methyl group to obtain a methyl triphosphate so that the system had a total charge of -2 e_0 in all three environments. Then, the vacuum energies of these structures were calculated by self-consistent field calculations in Gaussian03 (48) using B3LYP/6-31G*.

Experimental Setup for Difference Spectrum. Expression, purification, and FTIR measurements of the H-Ras 1–166 protein were performed as described previously (53). The sample solution for FTIR measurements contained 10 mM Ras 1–166, 200 mM 2-(*N*-morpholino)ethanesulfonic acid (pH 6.0), 20 mM $MgCl_2$, 20 mM dithiothreitol, and 0.1% glycol. Ras was loaded with the P3-1-(2-nitrophenyl)ethyl ester of GTP (caged GTP). The reaction was started by flashing the sample with a XeCl excimer laser. The difference spectrum between Ras•GTP and Ras•GDP was obtained by subtracting spectra collected before and after hydrolysis.

ACKNOWLEDGMENTS. We thank the Fund for Young Talents Frontier Project (2011KIP310), the Shanghai Institutes for Biological Sciences, and the Deutsche Forschungsgemeinschaft (SFB642) for financial support.

1. Vetter IR, Wittinghofer A (2001) Signal transduction: The guanine nucleotide-binding switch in three dimensions. *Science* 294:1299–1304.
2. Maegley KA, Admiraal SJ, Herschlag D (1996) Ras-catalyzed hydrolysis of GTP: A new perspective from model studies. *Proc Natl Acad Sci USA* 93:8160–8166.
3. Wittinghofer A, Waldmann H (2000) Ras: A molecular switch involved in tumor formation. *Angew Chem Int Ed Engl* 39:4192–4214.
4. Wittinghofer A, Vetter IR (2011) Structure-function relationships of the G domain, a canonical switch motif. *Annu Rev Biochem* 80:943–971.
5. Kötting C, Gerwert K (2004) Time-resolved FTIR studies provide activation free energy, activation enthalpy and activation entropy for GTPase reactions. *Chem Phys* 307:227–232.
6. Kötting C, et al. (2006) A phosphoryl transfer intermediate in the GTPase reaction of Ras in complex with its GTPase-activating protein. *Proc Natl Acad Sci USA* 103:13911–13916.
7. Langen R, Schweins T, Warshel A (1992) On the mechanism of guanosine triphosphate hydrolysis in ras p21 proteins. *Biochemistry* 31:8691–8696.
8. Futatsugi N, Hata M, Hoshino T, Tsuda M (1999) Ab initio study of the role of lysine 16 for the molecular switching mechanism of Ras protein p21. *Biophys J* 77:3287–3292.
9. Glennon TM, Villa J, Warshel A (2000) How does GAP catalyze the GTPase reaction of Ras? A computer simulation study. *Biochemistry* 39:9641–9651.
10. Kosztin I, Bruinsma R, O'Lague P, Schulten K (2002) Mechanical force generation by G proteins. *Proc Natl Acad Sci USA* 99:3575–3580.
11. Grant BJ, Gorfe AA, McCammon JA (2009) Ras conformational switching: Simulating nucleotide-dependent conformational transitions with accelerated molecular dynamics. *PLoS Comput Biol* 5:e1000325.
12. Shurki A, Warshel A (2004) Why does the Ras switch "break" by oncogenic mutations? *Proteins* 55:1–10.
13. Topol IA, Cachau RE, Nemukhin AV, Grigorenko BL, Burt SK (2004) Quantum chemical modeling of the GTP hydrolysis by the RAS-GAP protein complex. *BBA Proteins Proteom* 1700:125–136.
14. Grigorenko BL, Nemukhin AV, Topol IA, Cachau RE, Burt SK (2005) QM/MM modeling the Ras-GAP catalyzed hydrolysis of guanosine triphosphate. *Proteins* 60:495–503.
15. Klähn M, Braun-Sand S, Rosta E, Warshel A (2005) On possible pitfalls in ab initio quantum mechanics/molecular mechanics minimization approaches for studies of enzymatic reactions. *J Phys Chem B* 109:15645–15650.
16. Klähn M, Schlitter J, Gerwert K (2005) Theoretical IR spectroscopy based on QM/MM calculations provides changes in charge distribution, bond lengths, and bond angles of the GTP ligand induced by the Ras-protein. *Biophys J* 88:3829–3844.
17. Klähn M, Rosta E, Warshel A (2006) On the mechanism of hydrolysis of phosphate monoesters dianions in solutions and proteins. *J Am Chem Soc* 128:15310–15323.
18. Grigorenko BL, Nemukhin AV, Shadrina MS, Topol IA, Burt SK (2007) Mechanisms of guanosine triphosphate hydrolysis by Ras and Ras-GAP proteins as rationalized by ab initio QM/MM simulations. *Proteins* 66:456–466.
19. te Heesen H, Gerwert K, Schlitter J (2007) Role of the arginine finger in Ras-RasGAP revealed by QM/MM calculations. *FEBS Lett* 581:5677–5684.

20. Xia F, Rudack T, Kötting C, Schlitter J, Gerwert K (2011) The specific vibrational modes of GTP in solution and bound to Ras: A detailed theoretical analysis by QM/MM simulations. *Phys Chem Chem Phys* 13:21451–21460.
21. Lu Q, Nassar N, Wang J (2011) A mechanism of catalyzed GTP hydrolysis by Ras protein through magnesium ion. *Chem Phys Lett* 516:233–238.
22. Martin-Garcia F, Mendieta-Moreno JI, Lopez-Vinas E, Gomez-Puertas P, Mendieta J (2012) The role of GIn(61) in HRas GTP hydrolysis: A quantum mechanics/molecular mechanics study. *Biophys J* 102:152–157.
23. Milburn MV, et al. (1990) Molecular switch for signal transduction: Structural differences between active and inactive forms of protooncogenic Ras proteins. *Science* 247:939–945.
24. Pai EF, et al. (1990) Refined crystal structure of the triphosphate conformation of H-ras p21 at 1.35 A resolution: Implications for the mechanism of GTP hydrolysis. *EMBO J* 9:2351–2359.
25. Scheffzek K, et al. (1997) The Ras-RasGAP complex: Structural basis for GTPase activation and its loss in oncogenic Ras mutants. *Science* 277:333–338.
26. Scheidig AJ, Burmester C, Goody RS (1999) The pre-hydrolysis state of p21(ras) in complex with GTP: New insights into the role of water molecules in the GTP hydrolysis reaction of Ras-like proteins. *Struct Fold Des* 7:1311–1324.
27. Rosnizeck IC, et al. (2010) Stabilizing a weak binding state for effectors in the human Ras protein by cyclen complexes. *Angew Chem Int Edit* 49:3830–3833.
28. Rohrer M, et al. (2001) Structure of the metal-water complex in Ras center dot GDP studied by high-field EPR spectroscopy and P-31 NMR spectroscopy. *Biochemistry* 40:1884–1889.
29. Geyer M, et al. (1996) Conformational transitions in p21H-ras and in its complexes with the effector protein Raf-RBD and the GTPase activating protein GAP. *Biochemistry* 35:10308–10320.
30. Spoerner M, et al. (2010) Conformational states of human rat sarcoma (Ras) protein complexed with its natural ligand GTP and their role for effector interaction and GTP hydrolysis. *J Biol Chem* 285:39768–39778.
31. Wang JH, Xiao DG, Deng H, Callender R, Webb MR (1998) Vibrational study of phosphate modes in GDP and GTP and their interaction with magnesium in aqueous solution. *Biospectroscopy* 4:219–227.
32. Gerwert K (1999) Molecular reaction mechanisms of proteins monitored by time-resolved FTIR-spectroscopy. *Biol Chem* 380:931–935.
33. Kötting C, Kallenbach A, Suveyzdis Y, Wittinghofer A, Gerwert K (2008) The GAP arginine finger movement into the catalytic site of Ras increases the activation entropy. *Proc Natl Acad Sci USA* 105:6260–6265.
34. Troullier A, Gerwert K, Dupont Y (1996) A time-resolved Fourier transformed infrared difference spectroscopy study of the sarcoplasmic reticulum Ca^{2+}-ATPase: Kinetics of the high-affinity calcium binding at low temperature. *Biophys J* 71:2970–2983.
35. Cepus V, Ulbrich C, Allin C, Troullier A, Gerwert K (1998) Fourier transform infrared photolysis studies of caged compounds. *Methods Enzymol* 291:223–245.
36. Cepus V, Scheidig AJ, Goody RS, Gerwert K (1998) Time-resolved FTIR studies of the GTPase reaction of H-ras p21 reveal a key role for the beta-phosphate. *Biochemistry* 37:10263–10271.
37. Allin C, Gerwert K (2001) Ras catalyzes GTP hydrolysis by shifting negative charges from gamma- to beta-phosphate as revealed by time-resolved FTIR difference spectroscopy. *Biochemistry* 40:3037–3046.
38. Rudack T, Xia F, Schlitter J, Kötting C, Gerwert K (2012) The role of magnesium for geometry and charges in GTP hydrolysis, revealed by quantum mechanics/molecular mechanics simulations. *Biophys J* 103:293–302.
39. Takeuchi H, Murata H, Harada I (1988) Interaction of adenosine 5′-triphosphate with Mg^{2+}: Vibrational study of coordination sites by use of O-18-labeled triphosphates. *J Am Chem Soc* 110:392–397.
40. Pai EF, et al. (1989) Structure of the guanine-nucleotide-binding domain of the Ha-ras oncogene product p21 in the triphosphate conformation. *Nature* 341:209–214.
41. Warscheid B, et al. (2008) Systematic approach to group-specific isotopic labeling of proteins for vibrational spectroscopy. *Vib Spectrosc* 48:28–36.
42. Merrick JP, Moran D, Radom L (2007) An evaluation of harmonic vibrational frequency scale factors. *J Phys Chem A* 111:11683–11700.
43. Andersson MP, Uvdal P (2005) New scale factors for harmonic vibrational frequencies using the B3LYP density functional method with the triple-xi basis set 6-311+G(d,p). *J Phys Chem A* 109:2937–2941.
44. Sinha P, Boesch SE, Gu CM, Wheeler RA, Wilson AK (2004) Harmonic vibrational frequencies: Scaling factors for HF, B3LYP, and MP2 methods in combination with correlation consistent basis sets. *J Phys Chem A* 108:9213–9217.
45. Rudbeck ME, et al. (2009) Infrared spectrum of phosphoenol pyruvate: Computational and experimental studies. *J Phys Chem A* 113:2935–2942.
46. Hess B, Kutzner C, van der Spoel D, Lindahl E (2008) GROMACS 4: Algorithms for highly efficient, load-balanced, and scalable molecular simulation. *J Chem Theory Comput* 4:435–447.
47. Van der Spoel D, et al. (2005) Gromacs: Fast, flexible, and free. *J Comput Chem* 26:1701–1718.
48. Frisch MJ, et al. (2003) *Gaussian 03* (Gaussian Inc, Pittsburgh), B.04.
49. Groenhof G, et al. (2004) Photoactivation of the photoactive yellow protein: Why photon absorption triggers a trans-to-cis Isomerization of the chromophore in the protein. *J Am Chem Soc* 126:4228–4233.
50. The CPMD Consortium (1997) *CPMD* (IBM Corp/MPI für Festkörperforschung, Stuttgart).
51. Biswas PK, Gogonea V (2005) A regularized and renormalized electrostatic coupling Hamiltonian for hybrid quantum-mechanical-molecular-mechanical calculations. *J Chem Phys* 123:164114.
52. Höweler U (2007) *MAXIMOBY* (CHEOPS, Altenberge, Germany), 9.07.
53. Kötting C, Kallenbach A, Suveyzdis Y, Eichholz C, Gerwert K (2007) Surface change of Ras enabling effector binding monitored in real time at atomic resolution. *ChemBioChem* 8:781–787.